

# Chapter 1

## Modal Vibration Testing of a Frame and Wing Structure



Joshua E. Blackham and Matthew S. Allen

**Abstract** Large, multi-component bolted structures can exhibit complicated vibration responses due to the complexity of frictional interactions at the bolt-plate interface. The effect of nonlinearity due to the joints can be characterized by performing a test to quantify how the effective natural frequency and damping ratio of each mode change with vibration amplitude. In this paper, modal hammer impact testing was performed on the Round Robin Frame and Wing Structure. Various amplitude impacts were used to excite any nonlinearities in the structure. Experimental modal analysis was performed to separate the modal responses of the system. Mode shapes and frequencies are examined to understand any nonlinearities in the system.

**Keywords** Nonlinear Vibration · Experimental Modal Analysis · Frame and Wing Structure

### Introduction

The goal of modeling and testing complicated bolted structures is typically to create a model that can accurately replicate the effective natural frequency and damping of a test structure at the vibration amplitudes of interest. In order to make further progress in experimental-analytical substructuring, the Frame and Wing Structure (FWS) was introduced as a testbed structure that is relatively easy to model and test, with the ultimate goal of comparing and learning about different substructuring methods that are commonly used among different researchers and engineers [1].

Since the introduction of the Frame and Wing Structure, groups at Sandia have performed tests and modeled the structure. Moldenhauer and Roettgen [2] performed substructuring on the original FWS and were able to model the structure's mode frequencies and damping successfully. They also explored certain modes for large nonlinearities in the damping and found that most of the modes only exhibited weak nonlinearities. Linderholt et al. [3] also used substructuring to model the FWS, however, they modeled a new "swept" wing that represents a standard plane wing more accurately than the rectangular wing used in earlier models. Linderholt et al. [4] again modeled the FWS using substructuring methods. This time more complicated elements were added to the structure, such as vibration damping studs placed between the frame and the wing, or small payloads added on the wings. These elements were included in an attempt to introduce more nonlinearity into the system and to be able to model these changes through the developed substructuring processes.

While the original purpose of the frame wing project was to develop and compare different substructuring methods, this paper focuses on testing and characterizing the FWS. A roving impact test was performed to excite vibration modes from multiple locations and at various amplitudes. The frequency response functions (FRFs) obtained from both low-amplitude (i.e. assumed to be linear) responses and higher amplitude (i.e. nonlinear) responses were analyzed using the Algorithm of Mode Isolation to quantify the frequency and damping of each vibration mode. Mode shapes were also found and used to help explain any nonlinearities that might occur in each mode. The Hilbert transform [5, 6] was then applied to some of the high-amplitude impact data to quantify nonlinearities in the frequency and damping of certain modes.

---

Joshua E. Blackham

Department of Mechanical Engineering, Brigham Young University, Provo, UT 84601

e-mail: [joshblackham1925@gmail.com](mailto:joshblackham1925@gmail.com)

Matthew S. Allen

Department of Mechanical Engineering, Brigham Young University, Provo, UT 84601

e-mail: [matt.allen@byu.edu](mailto:matt.allen@byu.edu)

## Testing Procedure

The Frame and Wing Structure that was tested included both the frame component SN013 and the thin wing component Wing013A. For reference, the weights of the frame and wing components are 629.7 g and 527.7 g, respectively [7]. In this setup, the frame and wing components were attached using 4 10-32 bolts and #10 washers on each side of the frame as seen in Figure 1. The washers were placed only between the head of the bolt and the contact surface of the wing part. No nuts were used since the frame part was manufactured with threaded inserts placed in all bolt holes. All bolts were pretensioned to 3.4 Nm and the structure was suspended with bungees to approximate free-free boundary conditions. All rigid body modes of the suspended structure were found to be below 3 Hz, which was well below the first elastic mode of the structure.

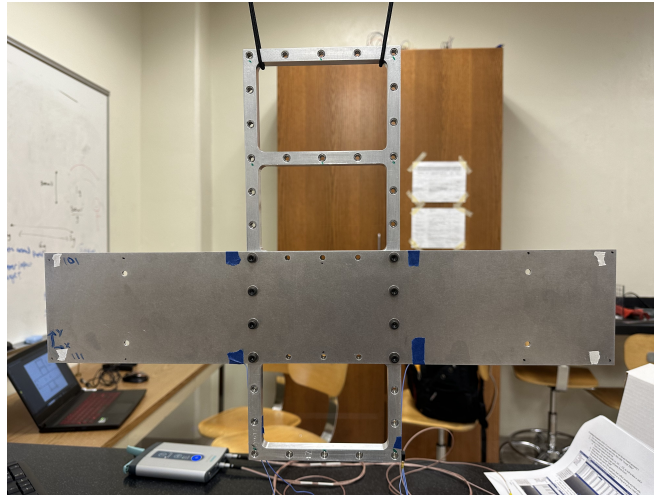


**Fig. 1** Frame and Wing structure suspended by bungees in preparation for modal impact testing

The goal of this testing was to characterize the mode frequencies and shapes of the frame and wing structure and to find modes that exhibit large nonlinearities due to the bolted joints. An initial round of testing focused on both low- and high-amplitude impact responses that were measured up to 1280 Hz. Low-amplitude impacts were used to find a baseline of linear mode frequencies and to find the mode shapes of the structure. High-amplitude impacts exercised the joint nonlinearity and hence could change the frequency and damping observed in a linearized FRF. The locations of the impact and accelerometers are shown in Figure 2, with 4 accelerometers positioned at the corners of the wing and one accelerometer on the frame. Note

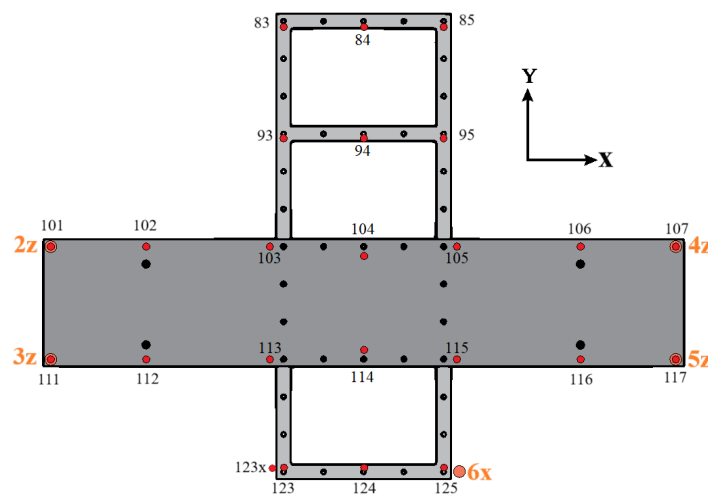


**Fig. 2** Locations of hammer impact points during testing. Impact locations are marked with red dots with a 2 or 3 digit numbering system. Unless specified, all impacts are in the Z direction. Accelerometers are located at points marked with orange circles and numbered 2-6 with directions specified.

that Accelerometer 6 was located on the side of the frame and oriented in the  $x$  direction in order to capture the response when impacts were performed in the X direction at Point 123. The impact locations extensively cover the length of the frame and wing parts and were chosen to allow the mode shapes to be found on both the frame and the wing components. After reviewing the initial testing, additional high-amplitude impacts were performed, which excited the structure up to about 700 Hz, in order to investigate nonlinear effects further.

## Frequency Response

The  $H_1$  FRF was computed from the impacts at low and high amplitudes and is shown in Figure 3. Figure 4 shows an expanded view for specific modes of interest. While investigating the corresponding mode shapes, the peak at 230 Hz exhibited unusual responses (see Figure 4c) and so two modes were suspected to exist at this frequency. The Complex Mode Indicator Function (CMIF) [8] was computed for the  $24 \times 5$  matrix of FRFs from the 5 accelerometers and 24 impact points, and the result is seen in Figure 5. The CMIF confirms that there are two modes that occur at 230 Hz as well as another pair near 650 Hz.

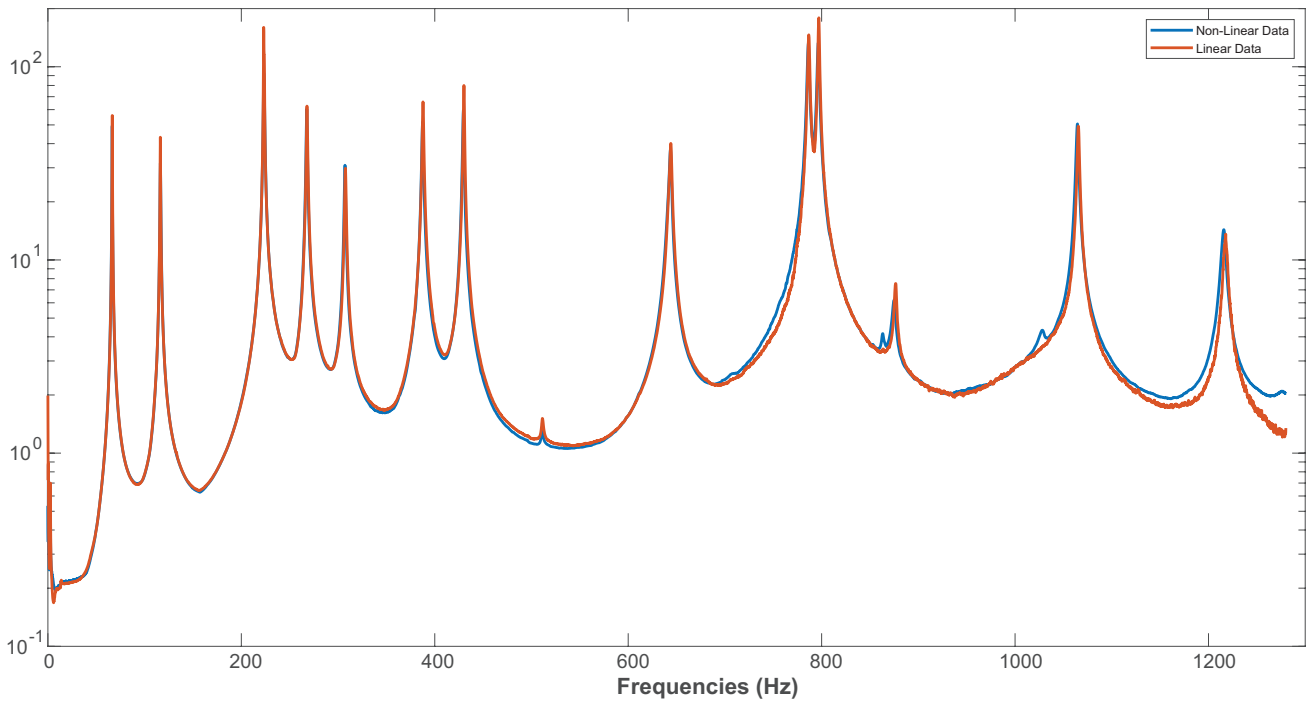


**Fig. 3** Comparison of average FRFs from low and high amplitude impact tests.

## Mode Frequencies and Shapes

After verifying the number of modes located at each frequency, the Algorithm of Mode Isolation (AMI) [9] was used to identify the modal parameters. In the cases where two modes occurred at about the same frequency, AMI used a two-mode fit to extract both modes from the measurements [10]. The mode frequencies and damping are summarized in Table 1, and the first eight mode shapes are seen in Figure 7. Modes 1, 2 and 7 (see Figs. 7a, 7b, and 7g) are predominantly wing bending modes. Modes 4 and 5 (see Figs. 7d and 7e) are frame bending modes with the wings undergoing torsion with Mode 4 in phase and Mode 5 out of phase. Modes 3 and 6 (see Figs. 7c and 7f) involve more complicated wing torsion modes and certain interactions between the wing and the frame. Mode 8 in Fig. 7h is a higher order wing bending mode that interacts with a frame torsion mode.

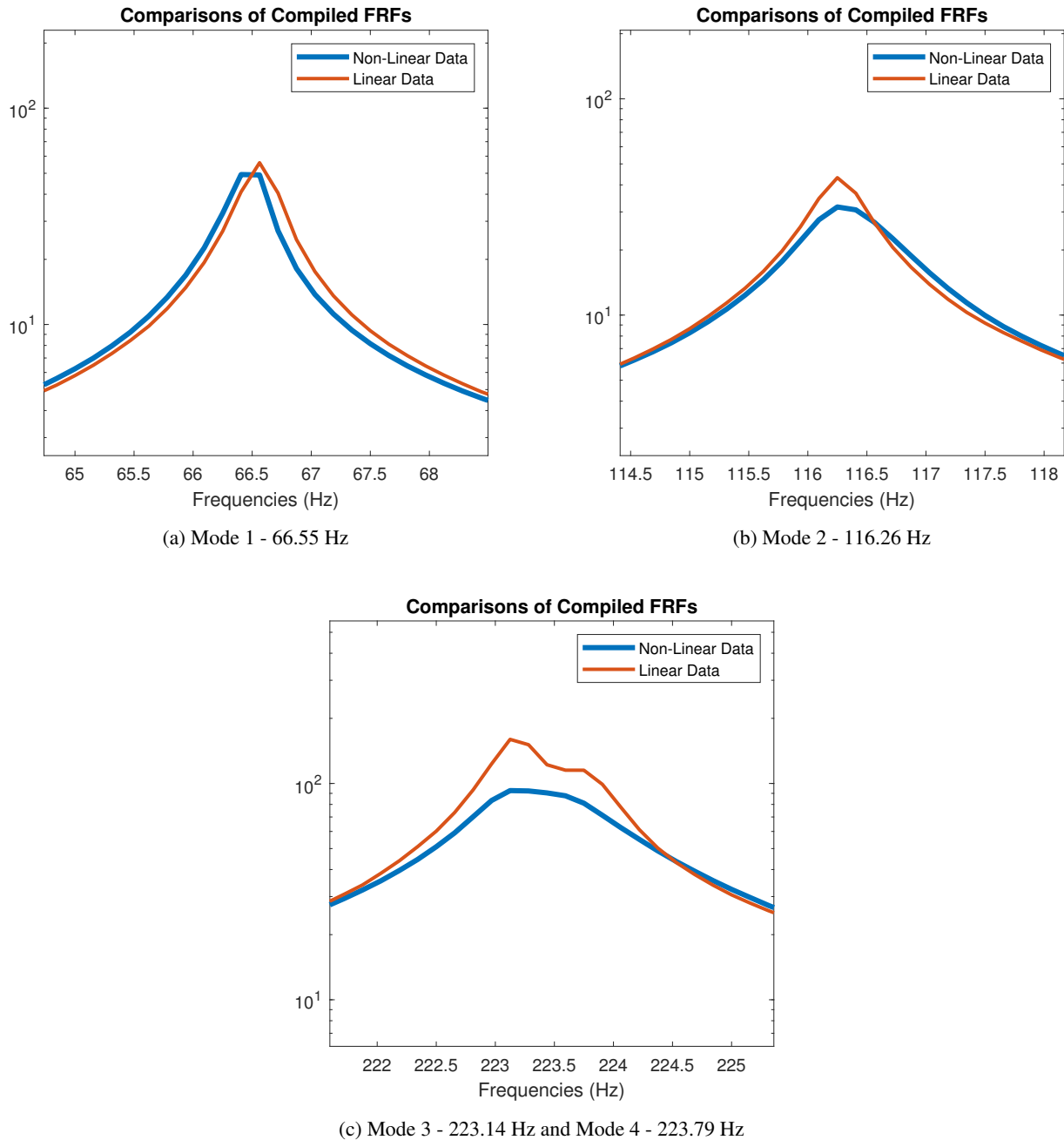


**Fig. 4** Zoom in on Frequency Response Function for the first 4 modes of the frame and wing structure

A few of the modes included in-plane motion. To identify these modes, the average of the FRFs for each of the accelerometers (i.e. the drive points) was plotted and is shown in Figure 6. Most of the modes are dominant in the accelerometers located on the wing and in the Z-direction (i.e. Acc. 2 - 5). The two exceptions are modes 9 and 14 at about 511 and 876 Hz, which are far more visible in the X-direction accelerometer 6 than in the Z-direction.

The plots of the mode shapes in Figure 7 can be used to ascertain which might be most sensitive to nonlinearity due to the bolted joints. For example, Mode 1 would exert a load that would want to open and close the bolted joints. This type of motion typically does not change the effective frequency or damping much [11], and the FRFs in Fig. 8 seem to support this. Mode 2 also shows little change in frequency or damping, and this seems to be corroborated by the fact that the mode shape

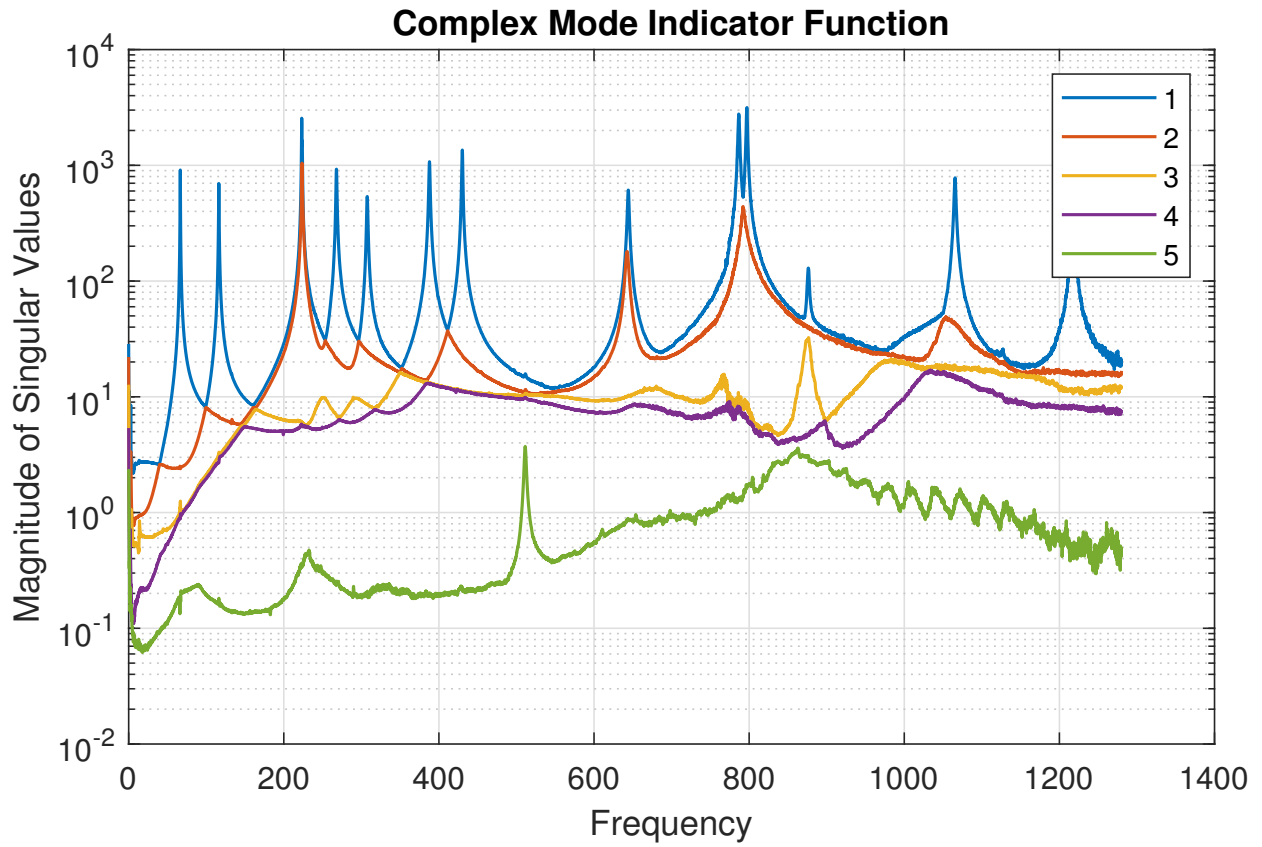


Fig. 5 Complex Mode Indicator Function for frame and wing low-amplitude impact test.

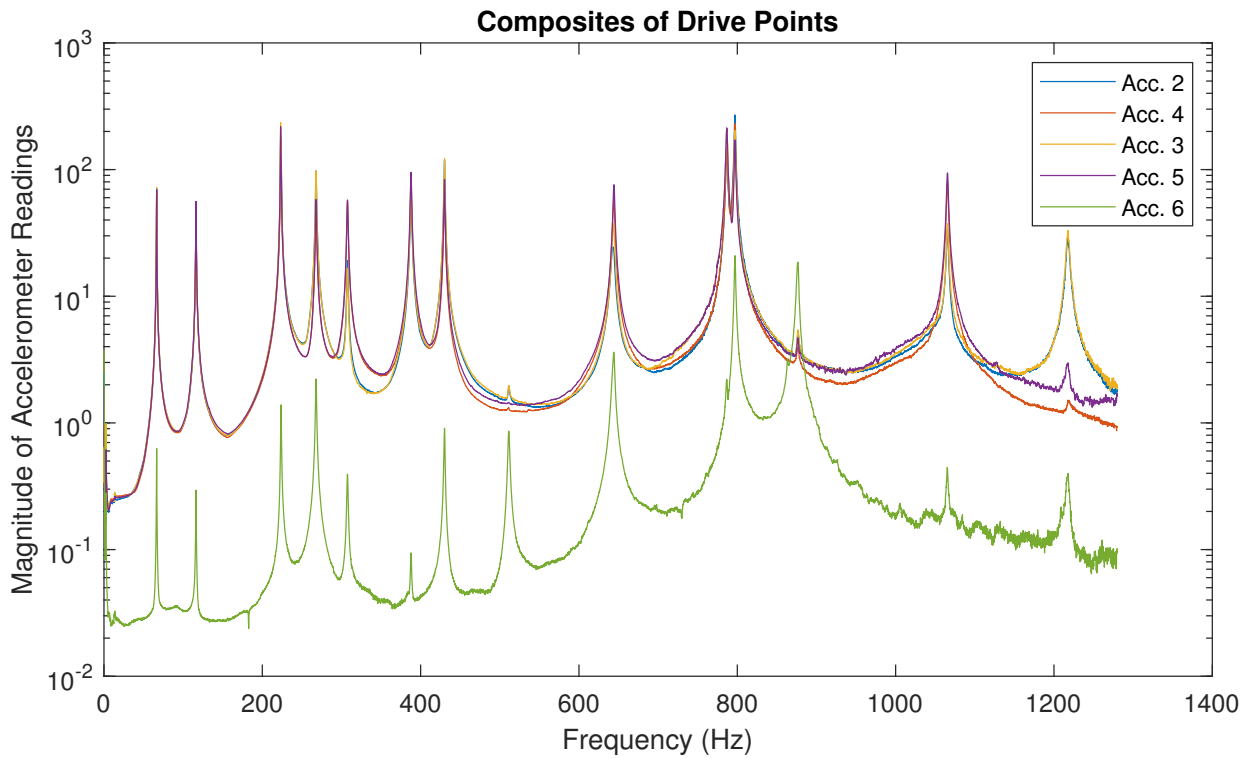
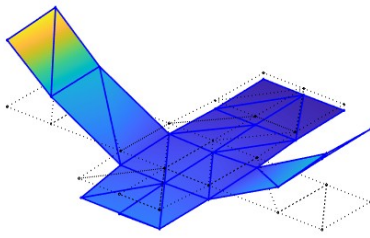
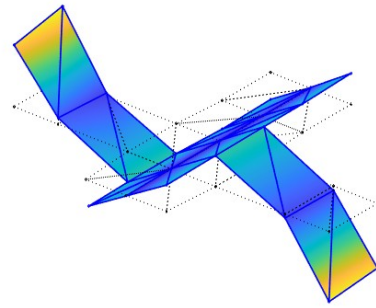


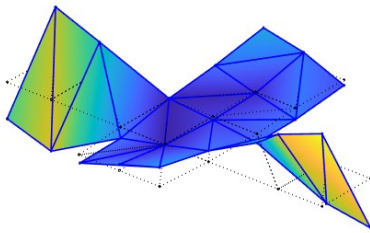
Fig. 6 Composite of drive points found using AMI.



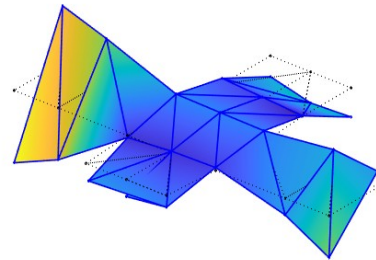
(a) Mode 1 - 66.55 Hz



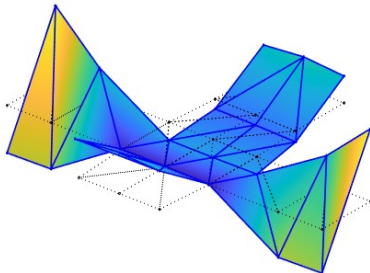
(b) Mode 2 - 116.26 Hz



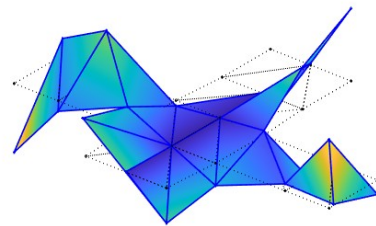
(c) Mode 3 - 223.14 Hz



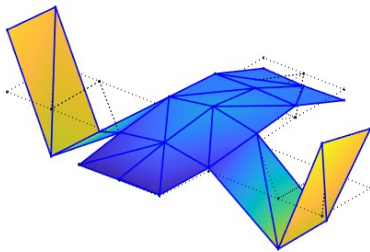
(d) Mode 4 - 223.79 Hz



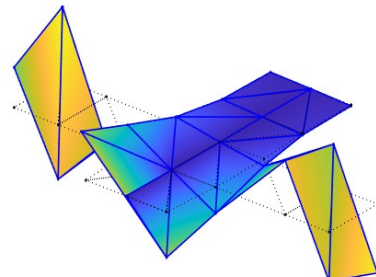
(e) Mode 5 - 267.88 Hz



(f) Mode 6 - 307.58 Hz



(g) Mode 7 - 387.83 Hz



(h) Mode 8 - 430.17 Hz

**Fig. 7** First eight Mode Shapes of Frame and Wing Structure

**Table 1** Mode frequencies and damping ratios of the frame and wing structure for low and high amplitude testing.

Mode	Description	Low Amp.		High Amp.		Difference	
		Freq. (Hz)	Damp. (%)	Freq. (Hz)	Damp. (%)	Freq. (%)	Damp. (%)
1	1st Wing Bending	66.55	0.24	66.46	0.22	-0.14	-8.3
2	2nd Wing Bending	116.26	0.22	116.33	0.33	0.06	50
3	1st Wing Torsion	223.14	0.10	223.12	0.23	-0.009	130
4	1st Frame Bending	223.79	0.15	223.67	0.23	-0.054	53
5	1st Frame Bending	267.88	0.22	267.66	0.23	-0.082	4.5
6	Torsion of Frame and Wing	307.58	0.24	307.16	0.22	-0.14	-8.3
7	3rd Wing Bending	387.83	0.19	387.39	0.21	-0.11	10
8	1st Frame Torsion	430.17	0.13	429.53	0.16	-0.15	23
9	In-Plane Mode 1	511.28	0.20	510.77	0.12	-0.10	-40
10	-	642.63	0.32	641.30	0.38	-0.21	19
11	-	644.18	0.16	643.73	0.17	-0.070	6.2
12	-	786.68	0.12	786.23	0.15	-0.057	25
13	-	797.01	0.09	796.45	0.14	-0.070	55
14	In-Plane Mode 2	876.25	0.14	874.50	0.21	-0.20	50
15	-	1065.4	0.10	1064.4	0.12	-0.094	20
16	-	1217.4	0.18	1215.6	0.20	-0.15	11

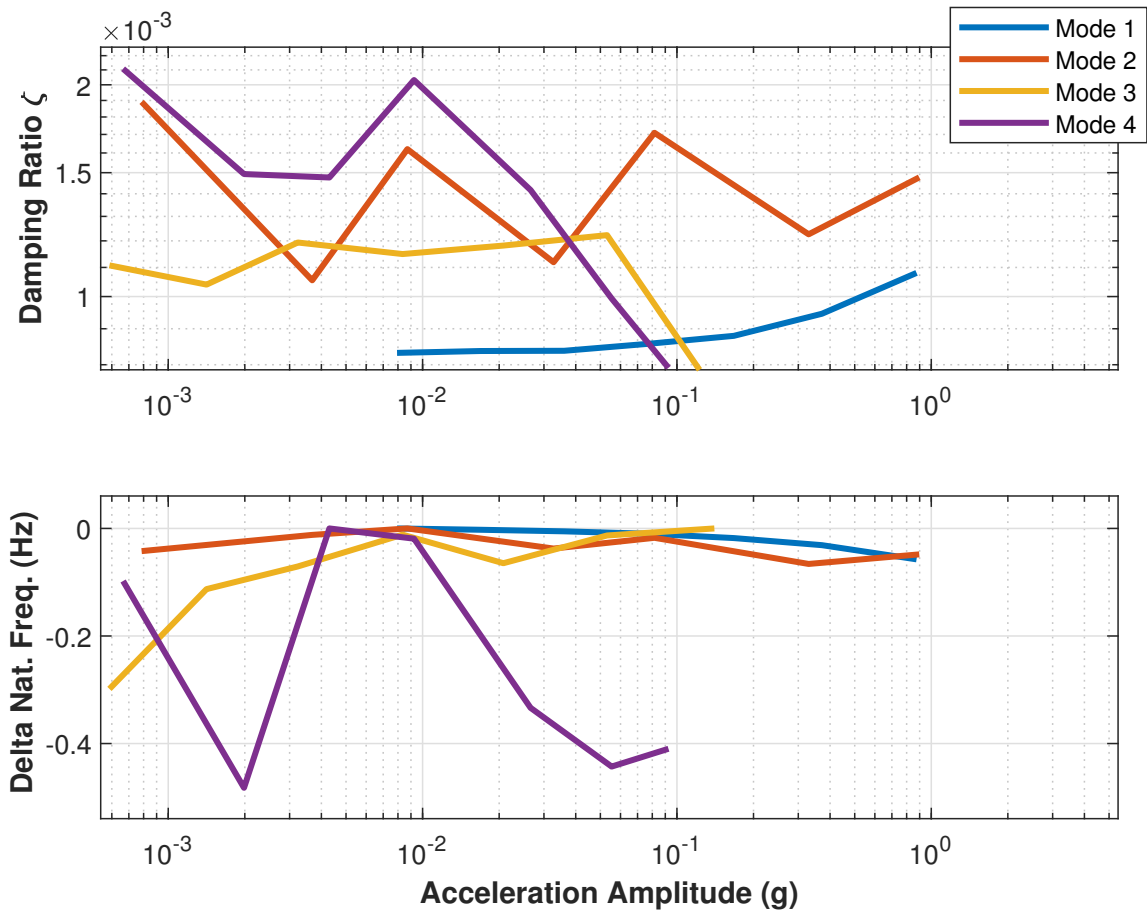


**Fig. 8** Amplitude dependent damping and frequency of the first 4 modes.

would not put much stress on the joints. This trend is similar for many of the bending and torsion modes of the structure. On the other hand, Modes 8 and 14 involve shearing of the joint, suggesting significant nonlinearity, and the results show that they exhibit somewhat larger than normal changes in frequency and damping. It should be noted, however, that these inferences based on the mode shapes are not infallible. For example, Modes 3 and 4 exhibit a relatively large increase in damping, even though their shapes mostly involve opening and closing of the joints as with most of the other modes. On the other hand, these modes are close in frequency so that may introduce error in estimating their damping. To ascertain which modes have nonlinear frequencies and damping, the Hilbert transform was used and will be discussed later.

## Hilbert Transform and Nonlinear Analysis

After mode frequencies and damping were found using AMI, the next step was to investigate any nonlinear effects that might occur due to the bolted joints and friction interfaces in the structure. First, a modal filter was used to separate the responses of the closely spaced pairs of modes. A band-pass filter was also used to obtain only the frequencies for specific modes of interest. After both filters were applied to the high amplitude impact data, the Hilbert transform was then used as described in [6] to find the amplitude dependent frequencies and damping for the first four modes and for Mode 9 of the frame and wing structure. The results are shown in Figs. 8 and 9.

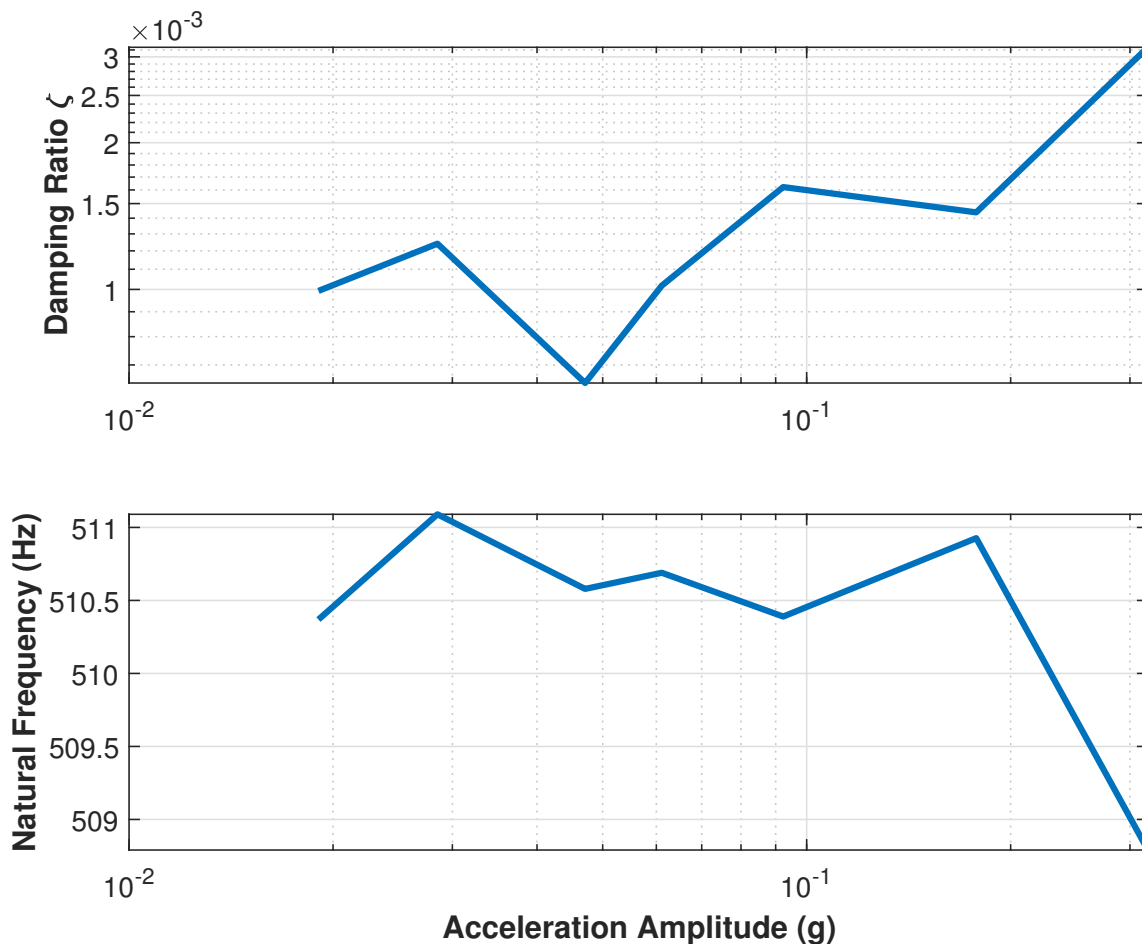


**Fig. 9** Amplitude dependent damping and frequency of Mode 9.

Mode 1 has the cleanest data in both damping and natural frequency and shows a small change across the amplitude range of interest. Such an increase in damping and decrease in stiffness is characteristic of structures with bolted-joint nonlinearities [12]. Mode 2 shows almost no change in natural frequency and a much noisier damping curve, however, the

general trend is that the damping is relatively unchanged as well. Modes 3 and 4 are the two modes that occur at the same frequency and so the assumptions that modal coupling does not occur may not have been met. This could be a possible explanation for the large amounts of noise in the Mode 4 curves. Overall, it seems that these four modes are predominantly linear across range of amplitudes that were accessible in these tests. Noisy results such as those shown in Fig. 8 are typical when applying this technique to data when the response is linear.

Figure 9 shows the nonlinear damping and natural frequency for Mode 9. Although slightly noisy, the damping increases by a factor of 3 as amplitude increases. The natural frequency has a less clear trend although the frequency does seem to drop by almost 2 Hz as amplitude increases. This type of response is typical for a nonlinear mode.

## Conclusion

In this paper, the Sandia Frame and Wing structure was tested to classify its vibration modes in order to understand the effect of bolted joints on the structure. Low amplitude hammer impact testing was performed to find the linear frequencies, damping and mode shapes. A second set of FRFs was obtained at higher force levels, to quickly screen for nonlinearity. Mode shapes were also presented to visualize the interaction between the wing and frame through the bolted joints. High amplitude hammer impacts yielded a greater range of amplitude dependent data. By using the Hilbert transform, the amplitude dependent frequency and damping of several modes was investigated. For this structure, nonlinearity was found have only a minor effect on the frequency and damping of the majority of modes in the structure. The fact that many of these modes are linear is notable since the purpose of this structure is to develop and compare different linear substructuring methods, and hence the frame seems well suited for this purpose.

Though the modes in this structure tend to predominantly linear, two pairs of modes were discovered that occur at almost the same frequency. Hence, care must be taken when treating those modes.

## References

1. Roettgen, D., Lopp, G., Jaramillo, A., and Moldenhauer, B. "Experimental Substructuring of the Dynamic Substructures Round-Robin Testbed". In Allen, M., D'Ambrogio, W., and Roettgen, D., editors, *Dynamic Substructures, Volume 4*, pages 119–123, Cham (2023) Springer International Publishing.
2. Moldenhauer, B. and Roettgen, D. "Nonlinear Substructuring of the Dynamic Substructures Technical Division Structure". In *41st International Modal Analysis Conference (IMAC XLI)*, Texas, USA (2023) Society for Experimental Mechanics.
3. Linderholt, A., Roettgen, D., and Moldenhauer, B. "Combining steel and aluminum components of the Benchmark Structure for the Technical Division on Dynamic Substructuring". In *41st International Modal Analysis Conference (IMAC XLI)*, Texas, USA (2023) Society for Experimental Mechanics.
4. Linderholt, A., Roettgen, D., and Moldenhauer, B. "Nonlinear Subcomponent Attachments for the Technical Division on Dynamic Substructuring Benchmark Structure". In *42nd International Modal Analysis Conference (IMAC XLII)*, Florida, USA (2024) Society for Experimental Mechanics.
5. Feldman, M. "Non-linear system vibration analysis using Hilbert transform—I. Free vibration analysis method 'Freevib'". *Mechanical Systems and Signal Processing*, 8(2):119–127 (1994)
6. Roettgen, D.R. and Allen, M.S. "Nonlinear characterization of a bolted, industrial structure using a modal framework". *Mechanical Systems and Signal Processing*, 84:152–170 (2017)
7. Dynamic Substructuring Focus Group. "SEM 4UF Measured Properties". SEM Wikis. Accessed: 2024-06-10. [Online.] Available: [https://wiki.sem.org/wiki/SEM\\_4UF\\_Measured\\_Properties](https://wiki.sem.org/wiki/SEM_4UF_Measured_Properties).
8. Shih, C.Y., Tsuei, Y.G., Allemang, R.J., and Brown, D.L. "Complex mode indication function and its applications to spatial domain parameter estimation". *Mechanical Systems and Signal Processing*, 2(4):367–377 (1988)
9. Allen, M.S. and Ginsberg, J.H. "A Global, Single-Input-Multi-Output (SIMO) Implementation of The Algorithm of Mode Isolation and Applications to Analytical and Experimental Data". *Mechanical Systems and Signal Processing*, 20:1090–1111 (2006)
10. Allen, M.S. and Ginsberg, J.H. "Global, Hybrid, MIMO Implementation of the Algorithm of Mode Isolation". In *23rd International Modal Analysis Conference (IMAC XXIII)*, Florida, USA (2005) Society for Experimental Mechanics.
11. Clark, Brennen, Allen, Matthew S., and Pacini, Benjamin. "Nonlinear Normal Modes and Response to Random Inputs of Systems with Bilinear Stiffness". *Journal of Sound and Vibration*, (Submitted April 2024) (2024)
12. Segalman, D.J., Gregory, D.L., Starr, M.J., Resor, B.R., Jew, M.D., Lauffer, J.P., and Ames, N.M. "Handbook on Dynamics of Jointed Structures". Technical report, Sandia National Laboratories, Albuquerque, NM 87185 (2009)

